ISSN 1063-7834, Physics of the Solid State, 2016, Vol. 58, No. 3, pp. 601–605. © Pleiades Publishing, Ltd., 2016.
Original Russian Text © K.A. Gonchar, A.V. Kondakova, Subhra Jana, V.Yu. Timoshenko, A.N. Vasiliev, 2016, published in Fizika Tverdogo Tela, 2016, Vol. 58, No. 3, pp. 585–589.

OPTICAL PROPERTIES

Investigation of Halloysite Nanotubes with Deposited Silver Nanoparticles by Methods of Optical Spectroscopy

K. A. Gonchar[a, b, *], **A. V. Kondakova**[a], **Subhra Jana**[c],
V. Yu. Timoshenko[a, d], **and A. N. Vasiliev**[a, b, e]

[a] Moscow State University, Moscow, 119992 Russia
[b] Ural Federal University named after the first President of Russia B.N. Yeltsin, ul. Mira 19, Yekaterinburg, 620002 Russia
[c] Department of Chemical, Biological & Macro-Molecular Sciences, S. N. Bose National Centre for Basic Sciences, Block-JD, Sector-III, Salt Lake, Kolkata-700098, India
[d] Tomsk State University, pr. Lenina 36, Tomsk, 634050 Russia
[e] National University of Science and Technology "MISiS," Leninskii pr. 4, Moscow, 119049 Russia
**e-mail: k.a.gonchar@gmail.com*

Received August 12, 2015

Abstract—Halloysite nanotube composites covered by silver nanoparticles with the average diameters of 5 nm and 9 nm have been studied by methods of optical spectroscopy of reflectance/transmittance and Raman spectroscopy. It has been established that silver significantly increases the light absorption by nanocomposites in the range of 300 to 700 nm with a maximum near 400 nm, especially for the samples with the nanoparticle size of 9 nm, which is explained by plasmonic effects. The optical absorption increases also in the long-wavelength spectral range, which seems to be due to the localized electronic states in an alumosilicate halloysite matrix after deposition of nanoparticles. Raman spectra of nanocomposites reveal intense scattering peaks at the local phonons, whose intensities are maxima for the samples with the silver nanoparticle sizes of 9 nm, which can be caused by plasmonic enhancement of the light scattering efficiency. The results show the ability to use halloysite nanotube nanocomposites in photonics and biomedicine.

DOI: 10.1134/S1063783416030112

1. INTRODUCTION

Halloysite is a clay mineral belonging to a subclass of phyllosilicates. Halloysite nanotubes (HNTs) is the dominating form of natural halloysite. Halloysite is close to kaolinite in its composition and is subjected to a chemical formula $Al_2Si_2O_5(OH)_4 \cdot nH_2O$ [1, 2]. Wrapping of the material into a tubular structure is caused by a mismatch in the periods of a tetragonal SiO_2 layer and adjacent Al_2O_3 layer with the octahedral structure [3, 4]. This results in the formation of a layered tubular HNT structure. The outer nanotube surface is covered by the Al–OH groups, while the Si–O–Si groups are located on the inner surface. There are, herewith, the positive and negative charges at the outer and inner surfaces, respectively [5, 6]. The surface is thus the potential area for deposition of particles [7–10]. There are actually several articles dedicated to the properties of HNTs covered by various nanoparticles, and their possible application to prevent corrosion, increase thermal stability, deliver drugs, and so on [1, 5, 11–13].

Deposition of metal particles, such as gold and silver, onto HNTs is of interest due to the ability to induce surface plasmonic resonance that can be used in surface-enhanced Raman scattering (SERS) [14]. SERS is a powerful probing method in biochemical applications for detection of small amounts of organic substances, due to its sensitivity and ability to be used in real-time operation [15]. It was shown in many articles that enhancement of the SERS signal is caused by an increase in the electromagnetic field strength in the so-called "hot points" which are located at the interface between metal particles.

In [16], the influence of dimensions and shape of gold particles at the HNTs surface on the plasmonic properties of the structures were studied, whereas, in [17], SERS was found in halloysites covered with gold nanoparticles. Nevertheless, corresponding studies of HNTs covered by silver nanoparticles have not yet been conducted.

This work is aimed at studying the optical properties of halloysite covered by silver nanoparticles, in order to detect the plasmonic properties.

Parameters of HNTs samples

Sample	Silver nanoparticle diameter, nm
A	–
B	5
C	9

2. EXPERIMENTAL

The halloysite samples prepared from natural raw material in accordance with the standard technique [1, 18] were used, as well as the modified HNTs samples covered by silver nanoparticles with the diameters of 5 and 9 nm and prepared in agreement with a method by analogue to that in [18]. The table shows the parameters and designations of the samples.

The structural properties of the HNTs were studied with transmission electron microscope (TEM). The total reflectance and transmittance spectra in the range of 200–1300 nm were measured on a Perkin Elmer Lambda 950 spectrophotometer equipped with an integrating sphere. Raman spectra were recorded on a Horiba HR 800 micro-Raman spectrometer using the continuous HeNe laser excitation at a wavelength of 633 nm (the irradiation power of 10 mW and the spot diameter of 12 μm) and on a Renishaw InVia micro-Raman spectrometer at the continuous Ar-laser excitation at a wavelength of 514 nm (the irradiation power of 25 mW and the spot diameter of 10 μm). The measurements were made at room temperature in air.

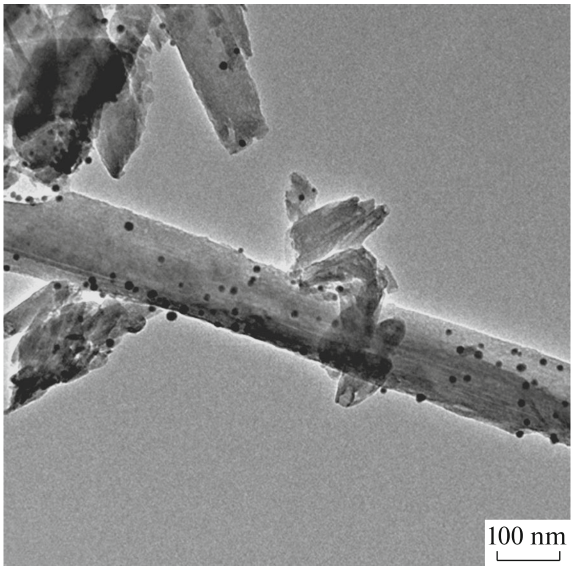

Fig. 1. TEM image of HNTs covered by silver nanoparticles.

3. RESULTS AND DISCUSSION

The electron microscopy study reveals that the halloysite samples are the cylindrical tubes composed of multi-layer walls with hollows (Fig. 1). Tubes length varies from 1 to 1.5 μm. The external tubes diameter is 50–100 nm, and the hollow size is about 15–20 nm. The observed defects on the HNTs surface can be related to the mechanical damages or crystal defects [19]. There are the silver nanoparticles at the nanotubes surface, whose diameters are 5 and 9 nm for various samples, and the distance between them is below 100 nm.

The reflectance (R) and transmittance (T) spectra were studied by means of an integrating sphere (Figs. 2a and 2b). As was established, the spectra of HNTs modified and covered by silver nanoparticles (samples B and C) are different from those of the initial HNTs (sample A). So, the reflection coefficient in the reflectance spectra for samples B and C is decreased in comparison with sample A (Fig. 2a). Herewith, sample C reveals a pronounced dip at a wavelength of 400 nm in addition to a reduction in the reflection coefficient, in contrast with sample A. An identical abrupt decrease at a 400-nm wavelength was also observed in the transmittance spectrum of sample C (in contrast with sample A). However, the light transmission coefficient has risen with increasing wavelength due to a decrease in the reflected radiation portion (Fig. 2b). Sample B showed considerably decreased reflection and transmission coefficients, unlike sample A.

Based on the reflection and transmission coefficients, the absorbance spectra (Abs) were plotted using a simple formula Abs = 1 – R – T (Fig. 2c). Obviously, the HNTs modified with silver nanoparticles (samples B and C) absorb stronger than the initial HNTs (sample A). Sample C exhibits a pronounced absorption peak at a wavelength of 400 nm, which is caused by the plasmonic resonance in silver nanoparticles [20]. With sample B, this absorption peak is much broader towards the long-wave spectral range. This broadening can be explained by the emergence of the collective modes that can arise when the silver nanoparticles do not touch, but are close to each other [21]. Usually, the broadening increases with a decrease in a distance between nanoparticles [22, 23]. Moreover, this absorption peak broadening can be due to a smaller diameter (5 nm) of silver nanoparticles, in contrast with sample C, which results in a more probable formation of their agglomerates and stronger oxidation. For these samples the increased absorption over the range of 400 to 700–750 nm can be related to both individual silver nanoparticles in the oxide environment and their agglomerates on the HNTs surface. Besides, the light absorption in the longer-wave spectral range can be attributed to the optical transitions between the local electronic state levels on the HNTs surface because of the presence of silver oxide.

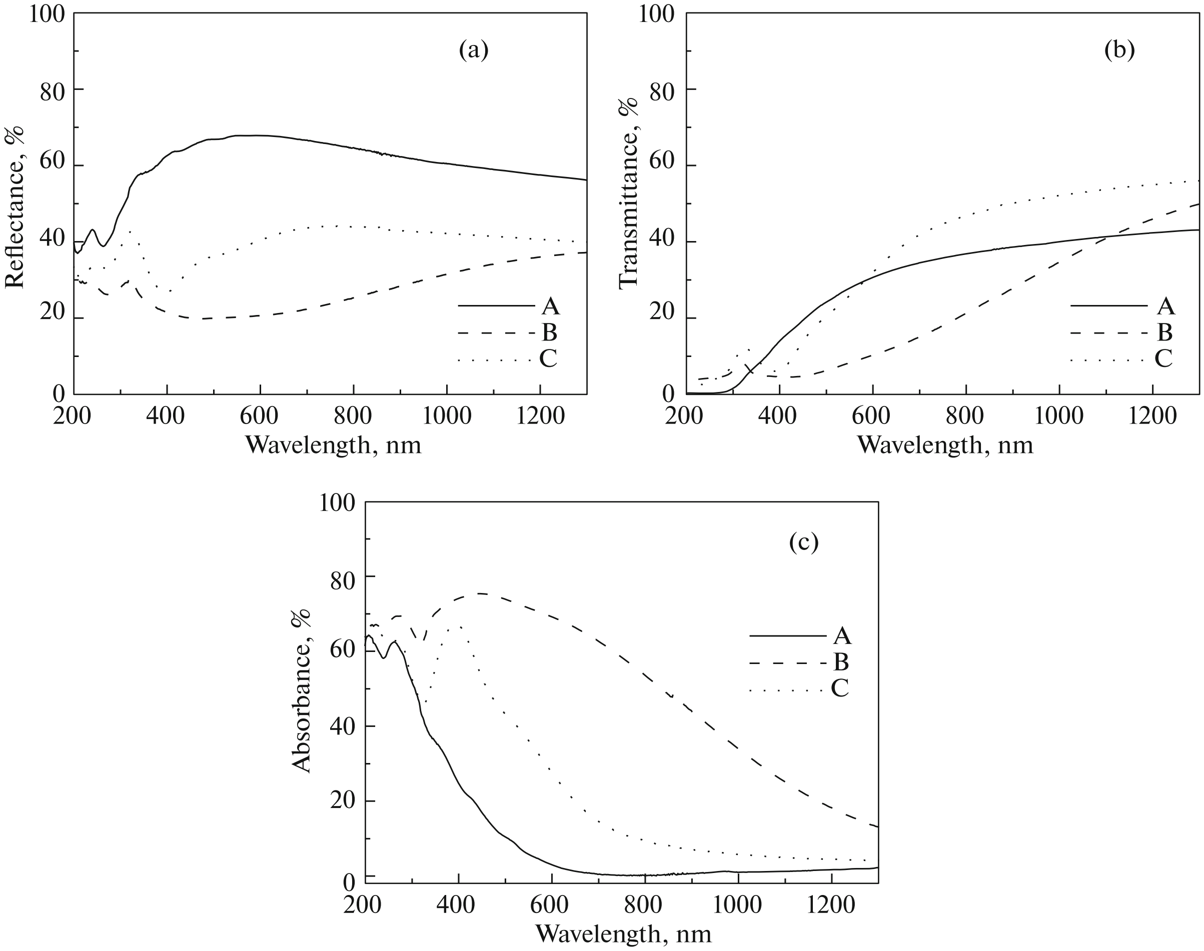

Fig. 2. (a) Reflectance, (b) transmittance, and (c) absorbance spectra of various HNTs samples.

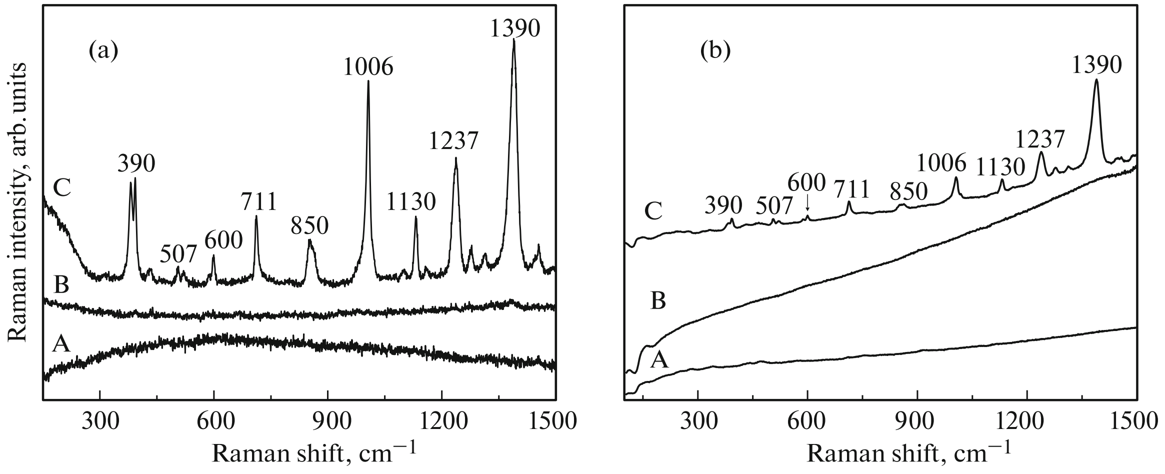

Fig. 3. Raman spectra of various HNTs samples at (a) 633 and (b) 514 nm laser excitation wavelengths. The spectra are spaced vertically for convenient representation.

Figures 3a and 3b display the Raman spectra at 633 nm and 514 nm laser excitation wavelength, respectively. The spectra are spaced vertically for the convenient representation. At the excitation of 633 nm the initial HNTs (sample A) exhibit the photoluminescence background with a maximum at 660 nm, which, however, weakens in the case of HNTs modified and covered by silver nanoparticles (samples B and C) (Fig. 3a). The pronounced Raman peaks were detected in sample C, which are attributed to halloysite [24, 25] and NH_2-groups, which are present in HNTs due to their modification and interaction with silver nanoparticles [26, 27]. No such effects were found in sample B, because the silver nanoparticles seem to be covered with an oxide layer due to their small diameters.

The photoluminescence background is also observed in a sample A at 514 nm excitation wavelength, which is enhanced in samples B and C (Fig. 3b). In addition, the same Raman lines are observed in sample C, as at a wavelength excitation of 633 nm. This fact testifies to the ability of Raman scattering enhancement in HNTs samples covered with silver nanoparticles due to the plasmonic properties of silver. The lack of the identical effects in sample B is explained by the small nanoparticle diameter, and the effect of the natural oxidation of silver is thus increased, which leads to a decrease in the metallic phase content.

4. CONCLUSIONS

In this work we studied the optical properties of HNTs covered with silver nanoparticles. The reflectance and transmittance spectra were measured using an integrating sphere, and the absorbance spectra were then plotted. As was established, the halloysites with 9-nm silver nanoparticles exhibit a plasmonic peak at a wavelength of 400 nm. The Raman spectra of these samples show the intensive lines attributed to local vibrational groups at the nanotubes surface, which means there is possibly plasmonic enhancement of the scattering processes by silver nanoparticles in such materials. No similar effects were observed in the HNTs covered with 5-nm silver nanoparticles, which seems to be due to the oxidation of silver.

The results on the formation of HNTs with deposited silver nanoparticles and the study of their optical properties show the ability to use these nanocomposites in photonics in order to enhance Raman scattering signals caused by the plasmonic effects that can be applied for spectroscopic analysis of various substances. Moreover, these nanocomposites can be used in biomedicine for antibacterial treatment of the surfaces of different objects and liquid media. One can thus expect both antibacterial influence of silver ions diffusing from immobilized nanoparticles and photocatalytic effect due to the excitation of plasmonic modes and, respectively, enhancement of local electric fields near silver nanoparticles. The observed broadening of a long-wave boundary of the plasmonic resonance in halloysite nanocomposites allows one to use not only ultraviolet radiation, but also the longer-wave range light, making their application particularly relevant.

ACKNOWLEDGMENTS

K.A. Gonchar is grateful to the Russian Scientific Foundation (project no. 15-12-20021); A.N. Vasiliev thanks the Ministry of Education and Science of the Russian Federation (project no. K2-2014-036 within the Program of MISiS).

The authors are grateful to Y.M. Lvov for useful discussion of the results and to A.A. Eliseev for help in the experiments.

REFERENCES

1. Y. Lvov and E. Abdullayev, Prog. Polym. Sci. **38**, 1690 (2013).
2. Y. Joo, Y. Jeon, S. U. Lee, J. H. Sim, J. Ryu, S. Lee, H. Lee, and D. Sohn, J. Phys. Chem. C **116**, 18230 (2012).
3. T. F. Bates, F. A. Hildebrand, and A. Swineford, Am. Mineral. **35**, 463 (1950).
4. B. Singh, Clays Clay Miner. **44**, 191 (1996).
5. E. Abdullayev, A. Joshi, W. Wei, Y. Zhao, and Y. Lvov, ACS Nano **6**, 7216 (2012).
6. G. Cavallaro, G. Lazzara, and S. Milioto, J. Phys. Chem. C **116**, 21932 (2012).
7. L. Wang, J. L. Chen, L. Ge, Z. H. Zhu, and V. Rudolph, Energy Fuels **25**, 3408 (2011).
8. M. X. Liu, B. C. Guo, M. L. Du, F. Chen, and D. M. Jia, Polymer **50**, 3022 (2009).
9. Yu. D. Tret'yakov, A. V. Lukashin, and A. A. Eliseev, Usp. Khim. **73**, 974 (2004).
10. I. V. Kolesnik, A. A. Eliseev, A. V. Garshev, A. V. Lukashin, and Yu. D. Tret'yakov, Russ. Chem. Bull. **53** (11), 2496 (2004).
11. E. Abdullayev, K. Sakakibara, K. Okamoto,W. Wei, K. Ariga, and Y. Lvov, ACS Appl. Mater. Interfaces **3**, 4040 (2011).
12. P. Yuan, D. Tan, and F. Annabi-Bergaya, Appl. Clay Sci. **112–113**, 75 (2015).
13. D. Rawtani and Y. K. Agrawal, Rev. Adv. Mater. Sci. **30**, 282 (2012).
14. I. R. Nabiev, R. G. Efremov, and G. D. Chumanov, Sov. Phys.—Usp. **31** (3), 241 (1988).
15. Y. Y. Jiang, X. J. Wu, Q. Li, J. J. Li, and D. S. Xu, Nanotechnology **22**, 385601 (2011).
16. M. Zieba, J. L. Hueso, M. Arruebo, G. Martinezab, and J. Santamaria, New J. Chem. **38**, 2037 (2014).
17. H. Zhu, M. L. Du, M. L. Zou, C. S. Xua, and Y. Q. Fu, Dalton Trans. **41**, 10465 (2012).
18. S. Jana and S. Das, RSC Adv. **4**, 34435 (2014).

19. P. Yuan, P. D. Southon, Z. Liu, M. E. R. Green, J. M. Hook, S. J. Antill, and C. J. Kepert, J. Phys. Chem. C **112**, 15742 (2008).
20. C. Diaz-Egea, R. Abargues, J. P. Martínez-Pastor, W. Sigle, P. A. van Aken, and S. I. Molina, Nanoscale Res. Lett. **10**, 310 (2015).
21. N. J. Halas, S. Lal, W.-S. Chang, S. Link, and P. Nordlander, Chem. Rev. **111**, 3913 (2011).
22. C.-Y. Tsai, J.-W. Lin, C.-Y. Wu, P.-T. Lin, T.-W. Lu, and P.-T. Lee, Nano Lett. **12**, 1648 (2012).
23. H. G. Duan, A. I. Fernández-Domínguez, M. Bosman, S. A. Maier, and J. K. W. Yang, Nano Lett. **12**, 1683 (2012).
24. R. L. Frost, Clays Clay Miner. **43**, 191 (1995).
25. R. L. Frost and H. E. Shurvell, Clays Clay Miner. **45**, 68 (1997).
26. M. R. Lopez-Ramirez, J. F. Arenas, J. C. Otero, and J. L. Castro, J. Raman Spectrosc. **35**, 390 (2004).
27. L.-B. Zhao, R. Huang, M.-X. Bai, D.-Y. Wu, and Z.-Q. Tian, J. Phys. Chem. C. **115**, 4174 (2011).

Translated by O. Maslova